摩擦学学报
TRIBOLOGY

遥爪型全氟聚醚自组装膜的表面性能及抗磨损和抗腐蚀性能研究

孟维晟，刘小龙，王海忠，乔旦，冯大鹏，宋增红，张坚，韩峰

Surface Properties, Wear Resistance, and Corrosion Resistance of TelechelicPerfluoropolyethersSelf-assembled Films

MENG Weisheng, LIU Xiaolong, WANG Haizhong, QIAO Dan, FENG Dapeng, SONG Zenghong, ZHANG Jian, HAN Feng

在线阅读 View online: https://doi.org/10.16078/j.tribology.2024123

孟维晟, 刘小龙, 王海忠, 乔旦, 冯大鹏, 宋增红, 张坚, 韩峰. 遥爪型全氟聚醚自组装膜的表面性能及抗磨损和抗腐蚀性能研究[J]. 摩擦学学报(中英文), 2025, 45(8): 1−11. MENG Weisheng, LIU Xiaolong, WANG Haizhong, QIAO Dan, FENG Dapeng, SONG Zenghong, ZHANG Jian, HAN Feng. Surface Properties, Wear Resistance, and Corrosion Resistance of TelechelicPerfluoropolyethersSelf-assembled Films[J]. Tribology, 2025, 45(8): 1−11. DOI: 10.16078/j.tribology.2024123

遥爪型全氟聚醚自组装膜的表面性能及抗磨损和抗腐蚀性能研究

孟维晟[1], 刘小龙[1], 王海忠[1*], 乔 旦[1], 冯大鹏[1*], 宋增红[2], 张 坚[2], 韩 峰[3]
(1. 中国科学院兰州化学物理研究所固体润滑国家重点实验室, 甘肃兰州 730000;
2. 山东东岳高分子材料有限公司含氟功能膜材料国家重点实验室, 山东淄博 256401;
3. 山东农业大学化学与材料科学院, 山东泰安 271000)

摘 要: 本文中以双端羧基Z型全氟聚醚为原料, 经还原和三甲氧基氯硅烷取代合成了具有双端硅氧烷基的两亲性Z型遥爪型全氟聚醚(PFSi, Mn≈10 000), 通过自组装, 将PFSi锚定于羟基化的硅片及铜片表面, 形成相应的膜. 考察了自组装膜的表面性能和耐磨损性能, 并探究了遥爪型全氟聚醚膜的抗腐蚀性能. 结果表明: PFSi自组装膜表现出较好地表面性能(表面张力＜10 mN/m). 同时, 经扫描电子显微镜观察, 硅片表面的自组装膜为多层结构. 加速磨损试验和电化学腐蚀试验表明: PFSi表现出优异的耐磨性能和耐腐蚀性能. 本工作中在制备具有耐磨损和耐腐蚀能力的低表面能膜的基础上, 研究了两亲性遥爪型聚合物在固体表面的自组装行为, 这将为设计可控自组装功能的含氟聚合物开辟一条新途径.

关键词: 全氟聚醚; 硅氧烷; 遥爪型聚合物; 多层结构; 自组装
中图分类号: TH117.1 **文献标志码:** A **文章编号:** 1004-0595(2025)08–0001–11

Surface Properties, Wear Resistance, and Corrosion Resistance of TelechelicPerfluoropolyethersSelf-assembled Films

MENG Weisheng[1], LIU Xiaolong[1], WANG Haizhong[1*], QIAO Dan[1], FENG Dapeng[1*], SONG Zenghong[2], ZHANG Jian[2], HAN Feng[3]

(*1. State Key Laboratory of Solid Lubrication, Lanzhou Institute of Chemical Physics, Chinese Academy of Sciences, Gansu Lanzhou 730000, China*
2. State Key Laboratory of Fluoride-Containing Functional Membrane Materials, Shandong Dongyue Polymer Materials Co, LTD., ShandongZibo 256401, China
3. School of Chemistry and Materials Science, Shandong Agricultural University, Shandong Tai 'an 271000 , China)

Abstract: In recent years, with the continuous acceleration of industrialization and urbanization, various equipment surfaces are frequently exposed to harsh environments and pollution sources, leading to an increasing demand for antifouling and corrosion resistance of material surfaces. As the complexity of demands and environments grows, traditional protective coating materials gradually prove inadequate. Therefore, it was highly significant to develop multifunctional composite coatings that possessed anti-fouling, wear-resistant, and corrosion-resistant properties.

Received 14 June 2024, revised 25 August 2024, accepted 26 August 2024, available online 28 August 2025.
*Corresponding author. E-mail: whzhlsl@licp.cas.cn, Tel: +86-931-4968170; E-mail: dpfeng@licp.cas.cn, Tel: +86-931-4968075.
The project was supported by the Shandong Natural Science Foundation Fluorosilicate Materials Mutual Fund(ZR2019LFG001, ZR2019LFG002 and ZR2019LFG009).
山东省自然科学基金氟硅材料联合基金项目(ZR2019LFG001, ZR2019LFG002, ZR2019LFG009)资助.

Polysiloxane and its modified materials primarily consist of silicone polymers or silicone-modified polymers as film material coatings. These materials exhibited exceptional thermal stability, weather resistance, chemical corrosion resistance, hydrophobicity, low surface energy, and excellent biocompatibility due to their unique valence bond structure. However, this structure also affected their wear resistance and oleophobic properties. Consequently, introducing both wear-resistant groups and amphiphobicity into organosilanes becomes necessary. In order to further enhance the antifouling capabilities as well as the wear- and corrosion-resistance of coating materials, In this study, amphiphilic Z-type telechelicperfluoropolyethers with double-terminated siloxanyl groups (PFSi, Mn≈10 000) were synthesized through a substitution reaction using potassium borohydride and trimethoxy-chlorosilane. The silicon and copper sheets were hydroxylated after cleaned and UV-Ozone treated, allowing for the growth of PFSi on their surfaces to form self-assembled films. The surface properties and wear resistance of the self-assembled film were investigated, along with the corrosion resistance of the remote claw type perfluoropolyether film. Results demonstrated that compared to pure silicon wafers, the PFSi self-assembled film significantly improved water repellency, diiodomethane repellency, seawater repellency, ethanol repellency and nonane repellency. Surface tension measurements using Owens two-liquid method revealed that the surface tension of PFSi self-assembled films at different concentrations was less than 10 mN/m. Scanning electron microscopy analysis showed that the self-assembled film on silicon wafer surfaces had a multi-layer structure with thickness increasing as concentration increases. Furthermore, accelerated wear tests indicated excellent wear resistance of the PFSi self-assembled film, which improved with higher concentration levels. Electrochemical corrosion tests also demonstrated effective prevention of corrosion factors on copper substrates by the PFSi self-assembled film thereby enhancing metal surface corrosion resistance. This study investigated the behavior of amphiphilic telechelicpolymers in solid surface self-assembly to develop low surface energy films with abrasion and corrosion resistance capabilities, thus providing a new approach for designing fluoropolymers with controllable self-assembly functions.

Key words: perfluoropolyethers; siloxane; telechelicpolymers; multi-layer structure; self-assemble

近年来，随着工业化和城市化进程的不断加快，各类设备的表面经常暴露在各种恶劣环境和污染源中，使得对材料表面的防污和耐蚀性需求日渐高涨. 伴随需求和环境的日益复杂性，传统的保护型涂层材料逐渐显现出不足，因此制备具有防污耐磨耐腐蚀的多功能复合涂层具有重要的意义[1-9]. 聚硅氧烷材料作为1种以有机硅聚合物或有机硅改性聚合物为主的膜物质涂层材料，近年来在性能改进及应用方面得到了迅速发展[10]. 有机硅烷通过水解能够形成高度交联的硬质网络，形成的聚硅烷涂层材料基于Si-O-Si价键结构使其具有优异的热稳定性、耐候性、耐化学腐蚀性、耐磨性、疏水性、低表面能及优异的生物相容性等特点[11-15]，但其特殊价键结构也使该材料存在强度低和与基材粘结性差等缺点. 通过将长烷基链、环氧化物、聚酯和聚氨酯等基团引入有机硅氧烷[15]，能够有效提高聚硅氧烷材料的强度和对基材的粘结性. 但该方法对涂层的耐磨性和疏油性有所降低[16-17]，因此需要将兼具耐磨性和双疏性的基团引入有机硅烷中，以进一步提高涂层材料的防污耐磨耐蚀性能.

全氟聚醚(PFPE)作为1种高性能润滑剂，一方面其能够通过含氟重复单元表现出低表面能、高热稳定性和化学惰性等特点[18-21]，另一方面在醚键的存在下表现出高韧性[22-23]. 得益于此，全氟聚醚在电子电气、汽车、纺织、航天工程和生命工程等诸多领域都有广泛应用. 例如，将端基为酰氟基的全氟聚醚衍生物通过自组装的方式接枝于羟基化的玻璃表面，其高浓度下自组装膜在展现出疏水性能的同时，还表现出优异的摩擦学性能和高的耐磨寿命[24]. 遥爪型聚合物作为1类通过中心聚合物链将两端基团或嵌段连接起来的聚合物，通常在选择性溶剂中表现出独特地自组装性质，在大多数情况下各嵌段部分都处于高度不对称状态，同时较短地嵌段主要位于聚合物链的外侧，这有利于分子间缔合形成交联[25-29]. 遥爪型聚合物这种主链两端功能化的结构可以保持聚合物主链结构独特的物理性质，同时其链端基团具有的交联特性，使其成为制备高弹性、自愈性和高透明性膜的复合材料[30-34].

结合遥爪型聚合物的自组装行为、全氟聚醚自身特殊性质以及硅氧烷在固体表面形成膜结构[35-37]的特点，推断将硅氧烷作为遥爪型聚合物的疏溶剂端基，必然会导致其在含氟溶剂中的疏溶剂作用显著增强，而这可能使该类遥爪型聚合物在固体表面形成独特结构.

因此，本文中设计并合成了由硅氧烷基构成全氟聚醚链两端端基的遥爪型含氟聚合物. 基于硅氧烷端基在含氟溶剂中的疏溶剂性质及在固体羟基表面自

组装的能力，由两亲性Z型遥爪型全氟聚醚（PFSi）所形成的膜具有优异的防污耐磨和耐腐蚀性能.

1　试验

1.1　试验材料

Z型全氟聚醚PF (Mn≈10 000)由山东东岳高分子材料有限公司提供，全氟环醚(FC-77)购自上海ACMEC，硼氢化钾(KBH_4)购自上海光明试剂厂，三甲氧基氯硅烷购自上海麦克林，乙醇和四氢呋喃购自天津利安隆.

1.2　遥爪型全氟聚醚的合成

以双羧酸基Z型全氟聚醚PF为原料，依次通过硼氢化钾还原及三甲氧基氯硅烷取代，合成制备了PFSi，具体合成路线如图1所示.

PFSi：取2 g (0.10 mmol)分子量为25 000的双端基Z全氟聚醚羧酸PF-1溶于10 mL全氟环醚(FC-77)后置于50 mL的圆底烧瓶中，依次加入20 mL四氢呋喃、10.92 mg (0.082 mmol)氯化锌与129.71 mg (2.41 mmol)硼氢化钾在65 ℃下反应8小时. 待反应结束，将粗产物经盐酸酸化、离心分离、真空旋蒸和冷冻干燥后获得中间还原产物PFOH-1. 将获得的PFOH-1置于50 mL的圆底烧瓶中，依次加入10 mL乙腈、10 mL全氟环醚、1 mL干燥三乙胺和30.14 mg (0.19 mmol)三甲氧基氯硅烷在室温下反应24小时. 待反应结束，将粗产物经真空旋蒸除去溶剂与未反应的三甲氧基氯硅烷后，获得无色透明的液体即为产物PFSi(1.92 g，产率96%). 红外光谱(KBr): 2 955(m), 2 926(m) [ν(-CH_3)], 2 856(m) [ν(-CH_2-)], 1 463(w), 1 402(w), 1 264(vs) [ν_{as}(-CF_2-)], 1 150(vs) [ν(Si-O-C)], 1 098(vs), 1 062(vs) [ν(-CF_2-)], 836(m), 815(m), 728(m), 687(m), 559(w), 534 cm^{-1}(w).

1.3　硅片与铜片表面自组装膜的制备

PFSi通过自组装方式在硅片和铜片表面生长成膜的过程如图2所示，具体步骤如下. 硅片表面预处理：将单晶硅片用石油醚和丙酮依次浸泡洗涤处理以除去表面附着的有机沉积物后，将其投入含有10%氢氟酸的水溶液中浸泡以除去表面的氧化层，再经去离子水洗涤和真空干燥得到表面干净的硅片.

铜片表面预处理：将铜片表面用砂纸打磨以除去表面氧化层，随后依次用无水乙醇、丙酮和石油醚浸泡洗涤以除去表面附着的碎屑和有机沉积物，干燥后得到表面干净的铜片.

硅片与铜片表面自组装膜的制备：将处理过的硅片和铜片在等离子清洗机中经UV-臭氧和等离子处理，使其表面羟基化；再将羟基化的硅片和铜片浸没于含有不同质量分数(1.0%、0.75%、0.50%和0.25%)双端Z型全氟聚醚硅氧烷的全氟环醚溶液中30 min，使含氟聚合物能够充分在硅片和铜片表面自组装生长，取出后浸没于甲醇/水(体积比90:10)溶液中并静置30 min，使表面生长的全氟聚醚的硅氧烷基水解以使表面的膜结构固定；最后将生长有全氟聚醚的硅片和铜片放入真空干燥箱中干燥.

1.4　试验仪器

使用ThermoFisherScientific型傅里叶变换红外光谱仪(FTIR)表征PFSi及其在硅片上的自组装薄膜. 使用DSA100接触角测量仪分别测量水、二碘甲烷、海

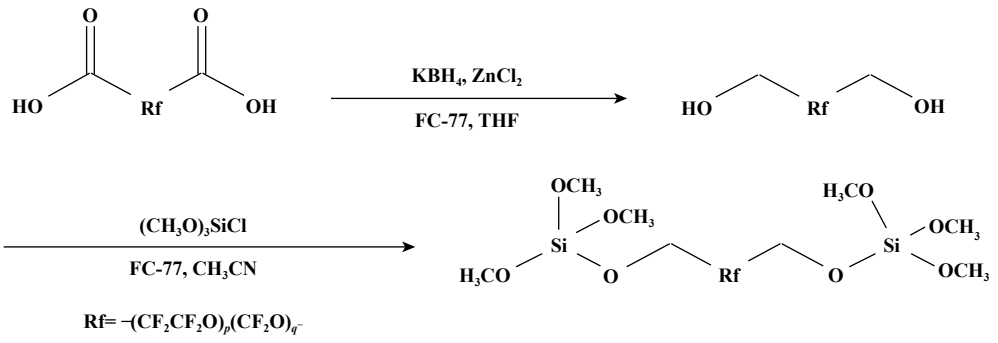

Fig. 1　Synthesis rout of the telechelic fluoropolymers

图 1　遥爪型含氟聚合物的合成路线

Fig. 2　Self-assembly film preparation process of telechelic polymer

图 2　遥爪型聚合物的自组装膜制备过程

水、乙醇和壬烷在PFSi自组装膜表面的接触角. 使用MS-9000摩擦试验机测试PFSi自组装膜的抗磨损性能. 使用JSM-5600LV型扫描电子显微镜(SEM)和VHX-6000超景深三维表面轮廓仪测量PFSi自组装膜形貌、表面磨斑形貌、氟含量和磨损量. 使用EMPYREAN高温原位材料结构分析系统通过X射线衍射(XRD)测试PFSi自组装膜表面的表面结构.

2 结果与分析

2.1 遥爪型全氟聚醚与其自组装膜的红外表征

图3所示为PFSi及其自组装膜的红外对比，红外光谱显示，相较于原料[图3(a)]，PFSi在1 781 cm^{-1}处归属于羧酸的伸缩振动峰消失，2 925和2 854 cm^{-1}处-CH_3和-CH_2-伸缩振动峰出现，这些峰为硅氧烷基的甲基及亚甲基的特征伸缩吸收峰；1 151 cm^{-1}处的强吸收带为Si-O-C伸缩振动峰，红外结果表明了PFSi的成功合成.

通过红外表征将生长有PFSi的硅片与纯硅片对比可以发现[图3(b)]，相较于纯硅片，1 046 cm^{-1}处C-F键的吸收峰强度有较大提升，表明硅片表面已生成含氟聚合物；同时2 923和2 851 cm^{-1}处-CH_2-的伸缩吸收峰出现，此为原PFPE链与硅氧烷连接处亚甲基残基的吸收峰. 这些吸收峰的出现表明PFSi已通过自组装方式在硅片表面生长形成膜结构.

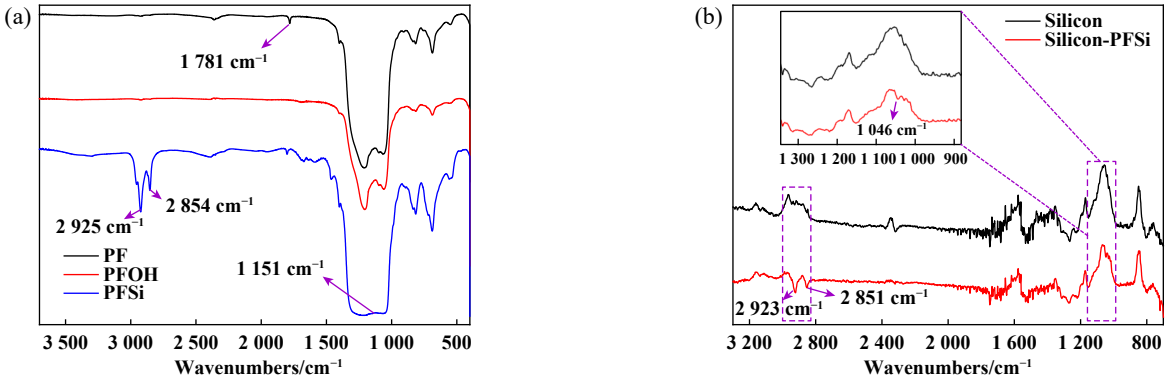

Fig. 3 Comparison of IR spectra : (a) PFSi; (b) the self-assembled films

图 3 红外光谱对比：(a) PFSi; (b) 自组装膜

2.2 自组装膜的表面性能研究

为测试表面接枝有遥爪型全氟聚醚硅片的表面性能，分别测试水和二碘甲烷的接触角及通过Owens二液法几何平均方程计算表面张力，表面张力计算公式如下.

$$r_L(1+\cos\theta) = 2(r_s^d \cdot r_L^d)^{1/2} + 2(r_S^p \cdot r_L^p)^{1/2} \quad (1)$$

$$r_S = r_S^d + r_S^p \quad (2)$$

其中，r_L为液体表面张力，r_L^d和r_L^p分别为色散分量和极性分量，θ为液体在固体表面上的接触角，r_S为固体表面张力，r_s^d和r_S^p分别为固体表面张力的色散分量和极性分量.

分别将2种已知液体的表面张力r_L和其分项r_L^d和r_L^p及接触角θ代入式(1)中，即可得包含2个独立方程的方程组，解此方程组便可求出r_s^d和r_S^p，进而由式(2)求出固体的表面张力.

在本试验中选择水和二碘甲烷作为测试液体，表面张力及色散分量和极性分量分别为：$r_{水}$=51 mN/m，$r_{水}^d$=21.8 mN/m，$r_{水}^p$=72.8 mN/m；$r_{二碘甲烷}$=2.3 mN/m，$r_{二碘甲烷}^d$=48.5 mN/m，$r_{二碘甲烷}^p$=50.8 mN/m.

测试及计算结果表明，与纯硅片相比，表面经PFSi处理过的硅片具有较大的水(>110°)和二碘甲烷(>99°)接触角，如图4(a)所示，其表面张力也随之降至9 mN/m，如图4(b)所示. 这得益于全氟聚醚分子链低表面能特性，使生长有PFSi的硅片获得双疏性能. 在以海水、乙醇和壬烷为测试液体的接触角测试中，表面生长有PFSi的硅片相比于纯硅片的接触角均表现出了显著提升，如图4(c)所示，表明PFSi能有效降低液体在硅片表面的润湿性，具有降低水溶性和油溶性污物在硅片表面附着的能力，使其具备了一定的防污性能. 此外，其优异的抗海水性能(CA>110°)能够有效防止电解质水溶液在硅片表面的附着，具有一定的防腐蚀能力. 但与水和海水相比，极性相对较小的乙醇和壬烷在PFSi表面具有较低的接触角，根据Fowkes模型[38]，表面张力被定义为极性和色散分项的总和，它们对表面张力的贡献决定了表面对极性和非极性液

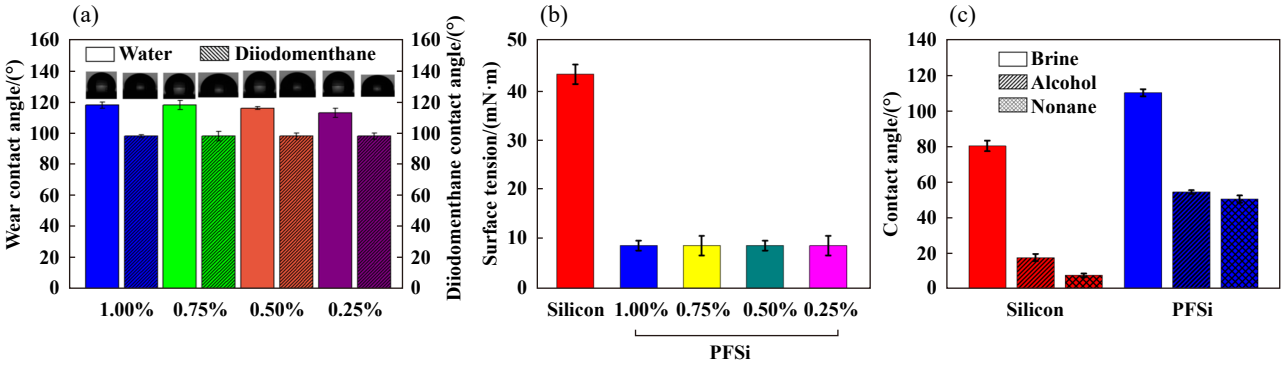

Fig. 4　Water and diiodomethane for PFSi: (a) the contact angles; (b)surface tension;(c) the contact angles of seawater, ethanol and nonane

图 4　(a) PFSi的水和二碘甲烷的接触角; (b)表面张力; (c)海水、乙醇和壬烷的接触角

体的亲和力. PFSi的色散分项(在1%质量分数下, r^d_{PFSi}=7.84 mN/m)远大于其极性分项(在1%质量分数下, r^d_{PFSi}=1.04 mN/m), 表明在遥爪型全氟聚醚端基烷基残基的参与下, 使表面生长有PFSi的硅片对低极性有机溶液的亲和力远高于极性液体.

2.3　自组装成膜形貌结构表征及成膜机理

图5所示为质量分数为1和0.25%的PFSi自组装膜的SEM照片, 利用扫描电子显微镜(SEM)观察硅片在质量分数为1%的PFSi中生长的自组装膜, 可以发现, PFSi自组装膜存在较明显的上下层分界现象, 如图5(a)所示, 上层表面相对较为平整, 下层存在较多颗粒状结构, 在两层的交界区也能够发现上下两层融合的现象, 表明PFSi在硅片表面的自组装结构可能通过逐层生长的方式实现, 且这一过程不受质量分数影响. 此外, 在接近自组装膜边缘部分存在与表面分离的卷曲层状结构, 如图5(b)和(c)所示, 对其内侧观察能够发

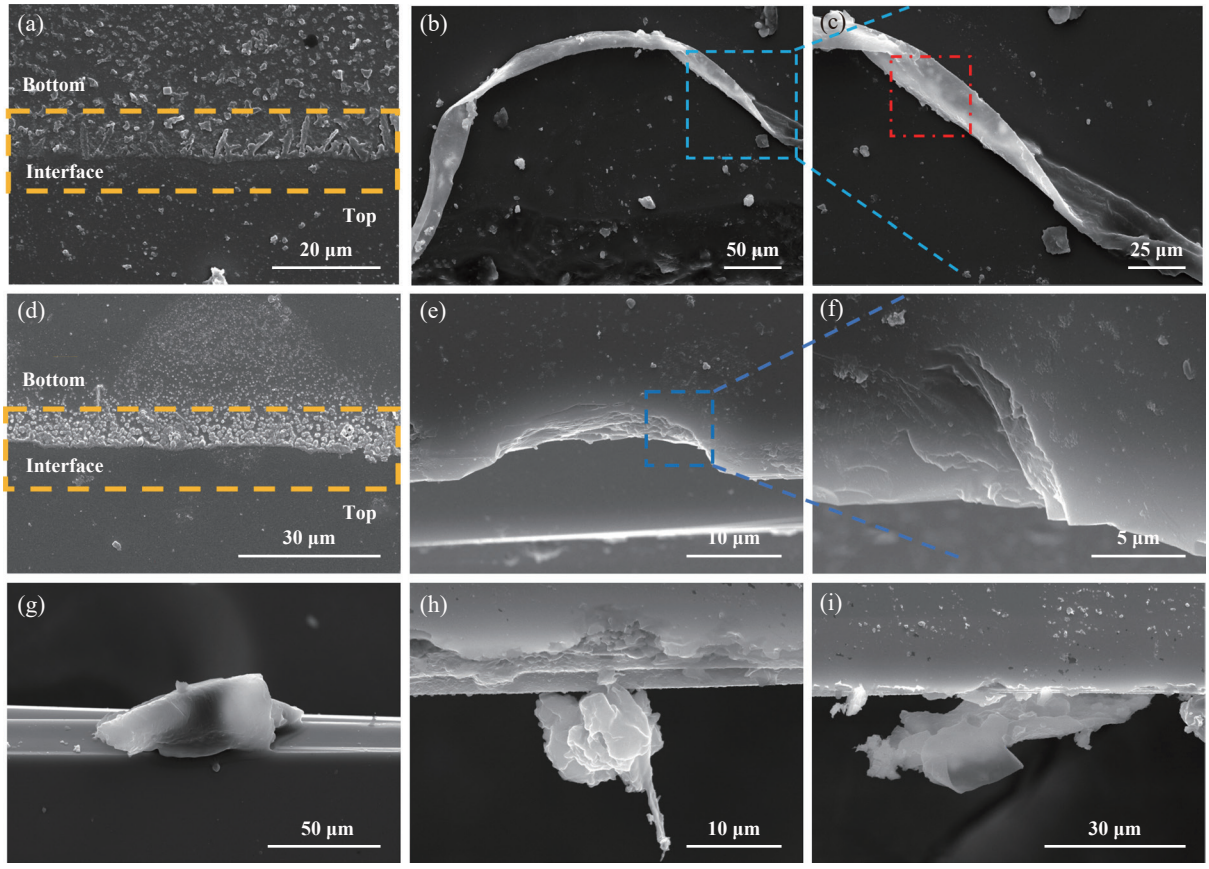

Fig. 5　SEM images of PFSi at concentration of self-assembled film: (a~c) 1%; (d~i) 0.25%

图 5　自组装膜PFSi的SEM图像: (a~c) 1%质量分数; (d~i) 0.25%质量分数

现类似多层结构残骸的片状凸起(红框处). 将PFSi的质量分数降至0.25%, 其自组装膜除能够观察到与质量分数为1%时类似的表面结构[图5(d)]外, 在其边缘处还存在较为明显的分层结构[图5(e~h)]、卷曲结构[图5(g)]和不规则多层堆积结构[图5(h~i]. 后2种结构与氧化硅自组织结构形貌相类似[39], 表明经羟基化处理的硅片对PFSi自组装膜的形成起到了一定的诱导作用, 使其能够在硅片表面沿垂直方向生长. 另外, 通过对硅片的截面观察能够发现全氟聚醚自组装膜的厚度存在随质量分数升高而增大的趋势, 如图6所示.

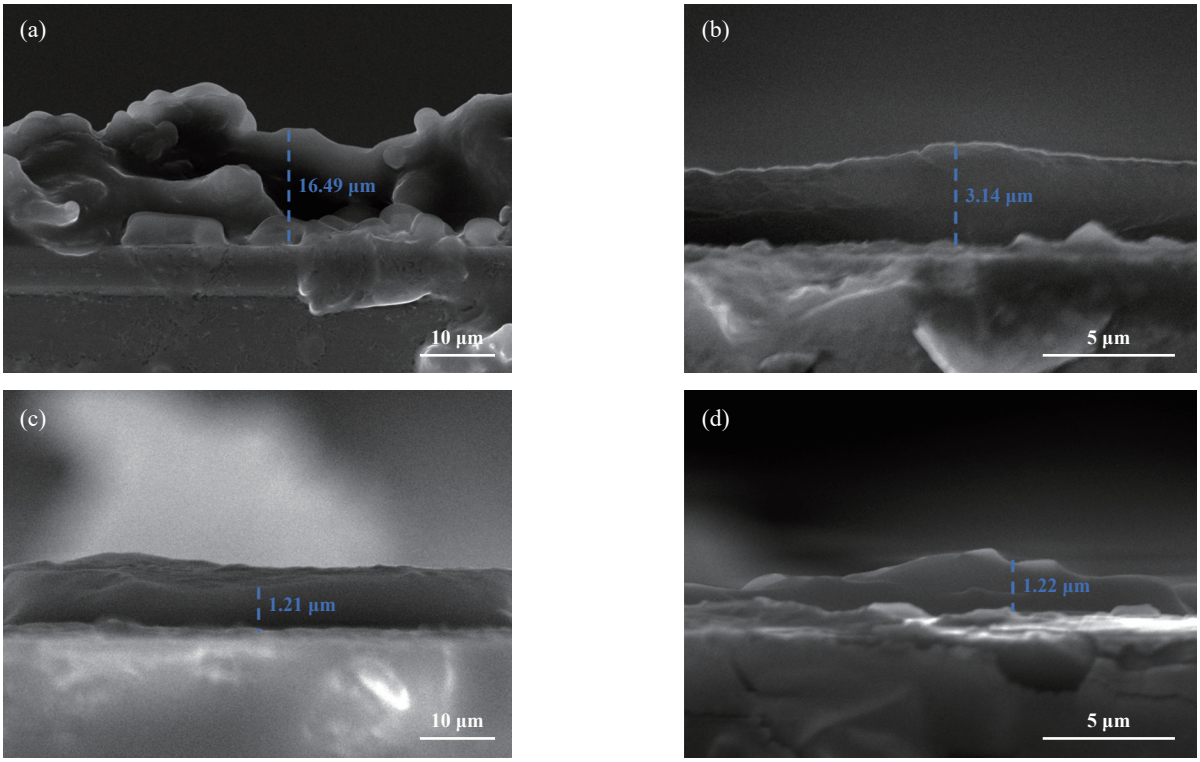

Fig. 6 SEM images of PFSi self-assembled film cross sections at concentrations of: (a) 1%; (b) 0.75%; (c) 0.5%; (d) 0.25%

图 6 质量分数为(a) 1%; (b) 0.75%; (c) 0.5%和(d) 0.25%的PFSi自组装膜截面的SEM照片

与含氟聚合物中心链相比, 全氟环醚相对于亲水的硅氧烷端基属于不良溶剂, 因此会影响PFSi在含氟溶剂中的结构[40-43]. 图7所示为遥爪型全氟聚醚膜在硅片表面自组装过程, 当羟基化的硅片浸入溶液后[图7(a)], 硅氧烷端基会优先与羟基通过水解反应, 使PFSi的一端锚定在硅片表面. 同时, 一方面由于中心全氟聚醚链张力的作用, 使另一端的硅氧烷端基无法通过中心链弯曲与硅片表面的羟基反应; 另一方面硅氧烷端基受到全氟环醚溶剂的疏溶剂作用影响, 使其倾向于吸引其他游离的硅氧烷基聚集以降低其亲水基团的曲率半径[43], 使分子沿全氟聚醚中心链伸展方向堆叠逐层生长[图7(b)和(d)]. 当将硅片浸入甲醇/水混合溶液后, 聚集的硅氧烷水解生成氧化硅刚性结构, 使自组装结构固定[图7(c), (e)和(f)][39], 故当通过SEM观察生长有PFSi的硅片时, 能够观察到分层现象. 正是基于PFSi在硅片表面这种逐层生长的性质, 质量分数对其表面张力的影响相对有限.

2.4 自组装膜磨损性能研究及抗磨损机理研究

通过加速磨损的方法[44]模拟由人类手指在触屏长期接触下对PFSi自组装膜的疏水性能变化及自组装膜的磨损寿命的影响. 使用由兰州华汇科技提供的MS-9 000多功能摩擦试验仪进行磨损试验, 使用等级为0000目的钢丝绒对测试硅片进行研磨, 如图8(a)所示. 钢丝绒与测试硅片完全接触, 在荷载的作用下钢丝绒对每个试样施加的平均垂直压力为20 kPa. 磨损探头的直径为1 cm, 每次磨损行程为2 mm, 频率为2 Hz, 载荷为2 N, 测试硅片平面尺寸为1 cm×1 cm.

藉由以上试验条件, 分别测试了不同质量分数PFSi自组装膜在3 000, 5 000和10 000次磨损试验下硅片表面的水接触角变化. 图8(b)所示为其测试结果, 结果表明经过3 000次摩擦后, 所有质量分数下PFSi的水接触角出现下降, 但水接触角依旧大于90°, 表明在钢

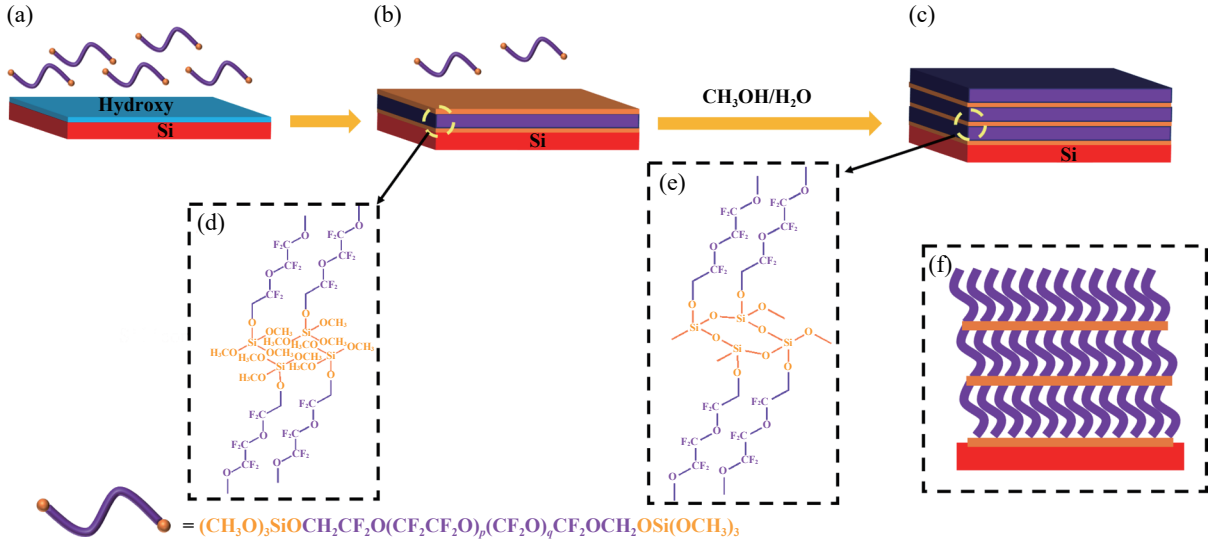

Fig. 7　The self-assembly process of telechelic perfluoropolyether films on the surface of silicon wafer

图 7　遥爪型全氟聚醚膜在硅片表面自组装过程示意图

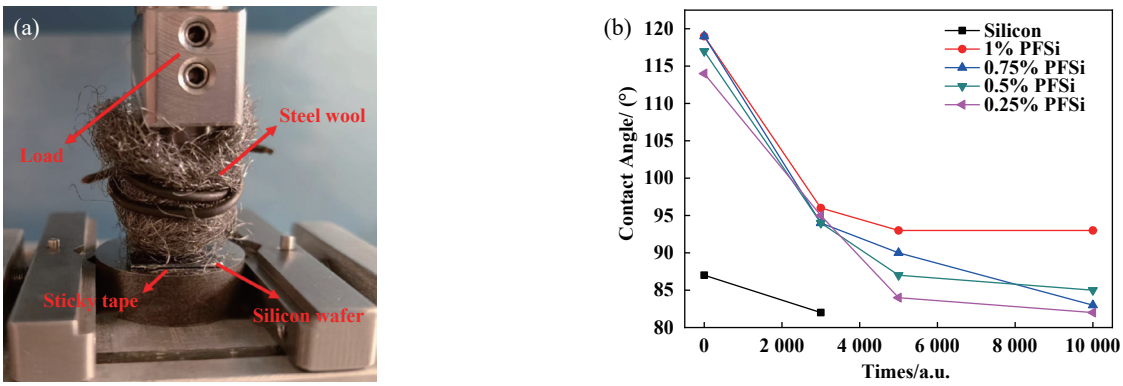

Fig. 8　(a)Simulated accelerated wear test equipment and(b) water contact angles of different friction times to the surface of the silicon wafer

图 8　(a)模拟加速磨损试验设备及(b)不同摩擦次数后的硅片表面的水接触角

丝绒摩擦破坏作用下，PFSi的多层结构能够有效保护硅片. 当摩擦次数达到5 000次时，质量分数低于0.5%的PFSi的硅片失去疏水能力，继续增大摩擦次数到10 000次，质量分数为0.75 %的硅片的水接触角与纯硅片接近，只有1%的PFSi-2能够在10 000次加速磨损后仍能保持其疏水能力，此外，通过对硅片表面磨损情况的观察可以发现，质量分数为1 %的PFSi在3 000次[图9(a~b)]和10 000次[图9(c~d)]磨损时，其表面的磨痕变化并不明显，磨斑形貌也以沟槽为主，并未观测到明显的固体结构成块脱落的现象，如图9所示. 这表明PFSi在高质量分数下形成的多层结构在较长时间的磨损破坏下能够维持其性能，因此，质量分数的提升有利于自组装结构的表面性能和磨损寿命.

结合磨损前后硅片表面结构及水接触角的变化可以发现，PFSi形成的多层结构能够提供较好的保护[45]如图10所示，一方面Si-O-Si刚性骨架在摩擦过程中起到一定的保护作用，降低钢丝绒对全氟聚醚层的冲击；另一方面，当多层结构的表层被破坏后，其下层相对完整的结构能够为硅片提供保护，同时残存的全氟聚醚链继续维持其表面疏水的能力. 此外，PFSi质量分数降低只会影响多层膜的厚度，因此不同质量分数下PFSi磨损后的水接触角变化较为显著. 在两亲性遥爪型聚合物自组装结构的影响下，PFSi形成的多层膜结构能够有效保护固体表面，提高固体表面的耐磨损性能. 此外，XRD显示Si-O键键长随PFSi质量分数增大而减小，如图11所示，这一变化进一步提高了自组装膜的耐磨性.

2.5　自组装膜的电化学行为

通过考察电化学行为以研究全氟聚醚自组装膜的耐蚀性能. 使用电化学工作站在3.5 % NaCl溶液中

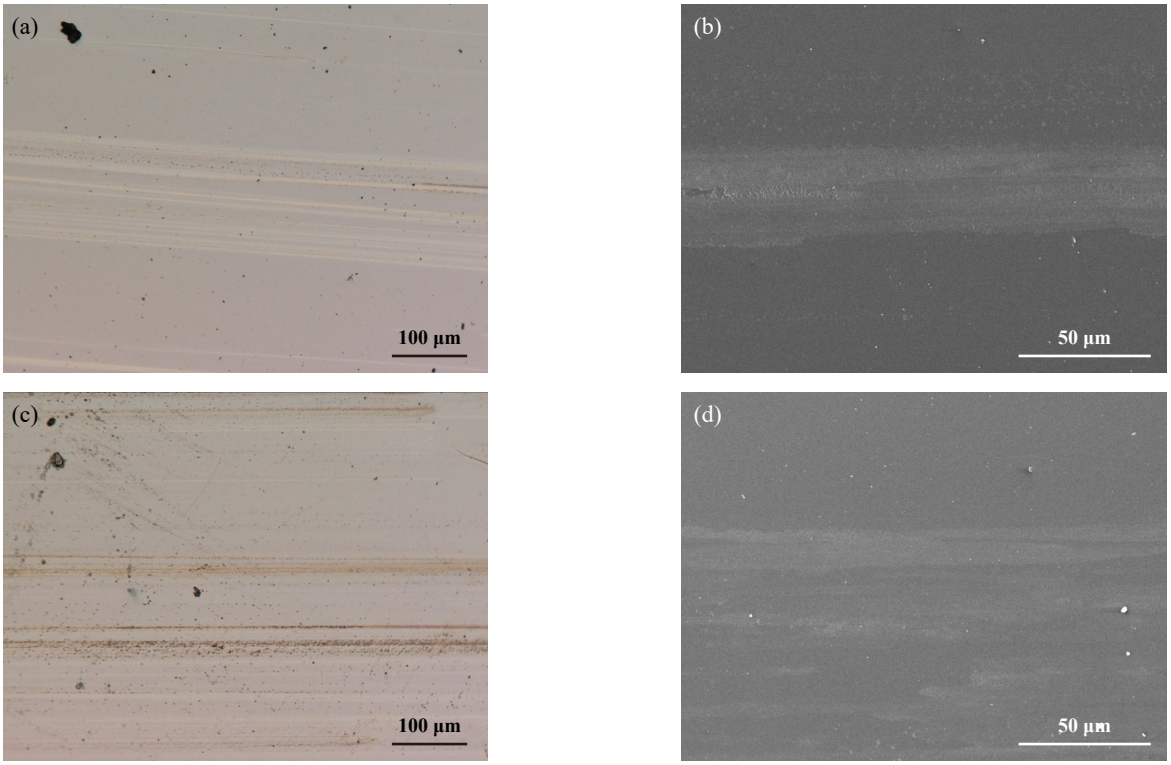

Fig. 9 Surface wear and SEM morphology of PFSi with a concentration of 1% at: (a, b) 3 000 times and (c, d)10 000 times

图 9 磨损对质量分数为1 %的PFSi在:(a, b) 3 000次和(c, d) 10 000次的表面磨损情况、SEM照片

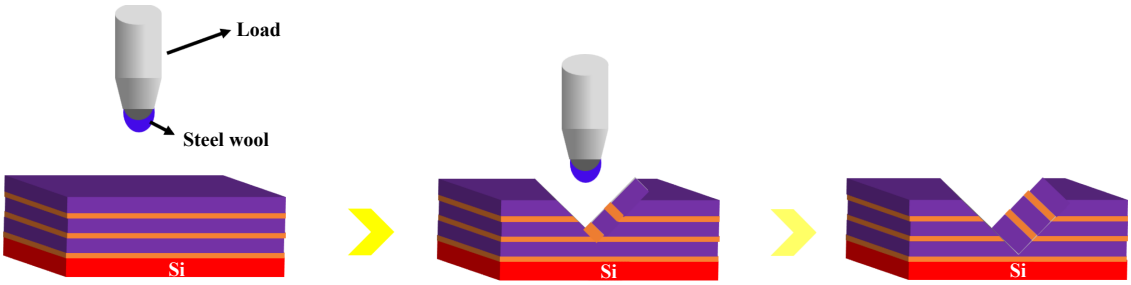

Fig. 10 The effect of wear on the surface structure of PFSi

图 10 磨损对PFSi表面结构影响的示意图

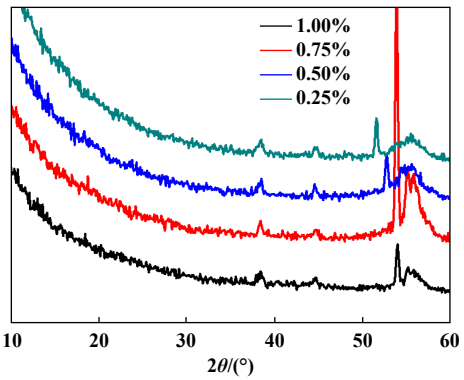

Fig. 11 XRD of PFSi self-assembled films at different concentrations

图 11 不同质量分数下PFSi自组装膜的XRD

测试空白铜片与表面生长PFSi的铜片的防腐蚀性能. 以铜片为工作电极，铂为对电极，Ag/AgCl电极(饱和KCl)为参比电极. 当开路电位处于平稳状态时，测量电极的电化学阻抗与Tafel曲线. 测量阻抗的频率范围为10^{-2} Hz ~10^{4} Hz，信号振幅为2 mV. Tafel极化曲线的扫描速率为2 mV/s.

图12(a)所示为空白铜片与生长有PFSi铜片在腐蚀环境下的Tafel极化曲线. 空白铜片的腐蚀电位为0.123 V. 比较而言，生长有PFSi的铜片的腐蚀电位提高至0.174 V，表明PFSi使铜片具有较低的腐蚀倾向. 此外，对比空白铜片，生长有全氟聚醚膜的铜片的腐蚀电流(1.10×10^{-8} A/cm^2)比空白铜片(7.24×10^{-8} A/cm^2)

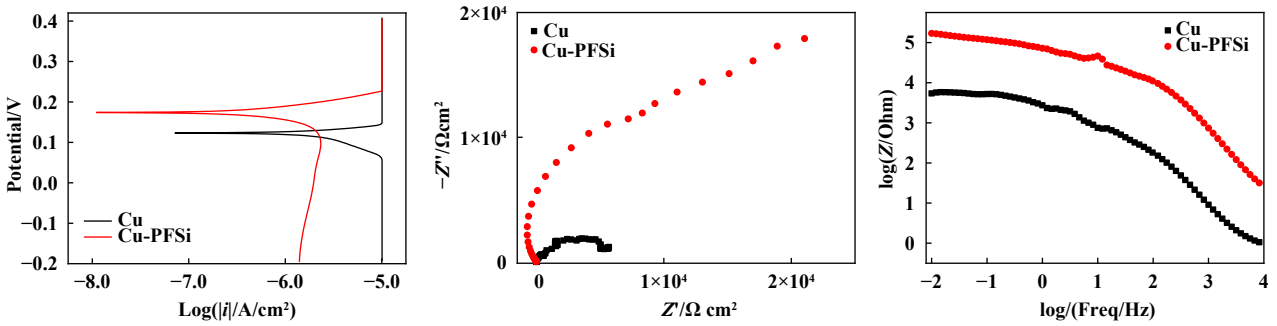

Fig. 12　(a) The Tafel curves, (b) Nyquist curves and (c) Bode curves of PFSi and copper

图 12　PFSi与纯铜片的(a) Tafel曲线、(b) Nyquist曲线和(c) Bode曲线

降低近7倍，腐蚀电流越小，腐蚀速率越低[46-47]，说明PFSi能够降低铜片表面的腐蚀速率，对腐蚀离子具有一定的阻挡能力. 其主要是由于全氟聚醚的疏水性质，减少腐蚀液体与铜片的接触面积，从而阻止腐蚀离子的渗入.

除了通过Tafel极化曲线分析空白铜片和生长有PFSi的铜片的腐蚀动力学，还考察了两者表面的电化学阻抗谱的变化，以评价全氟聚醚自组装膜的防腐性能和揭示腐蚀机理. 在Nyquist图中空白铜片表现为1个小的半圆弧，说明腐蚀离子已经渗入金属基底，腐蚀已经发生，如图12(b)所示. 相比之下，生长有PFSi的铜片的Nyquist图在高频区有较大的容抗弧，而在低频区具有1个Warburg阻抗，说明耐蚀性得到提高，PFSi在铜片表面形成较厚且致密的钝化膜，由于膜电阻很大，腐蚀离子迁移过程受到极大的抑制. 此外，Bode图中PFSi在低频区的阻抗值远大于空白铜片，如图12(c)所示，进一步表明PFSi具有良好的耐蚀性[48].

3　结论

本研究中以三甲氧基氯硅烷作为硅源合成了PFSi，并对其相应的理化性能进行了表征. PFSi能够在全氟环醚中通过自组装的方式在羟基化的硅片和铜片表面形成自组装膜. 形成的膜具有较好的疏水疏油性能和较低的表面张力，使其具有一定的防污性能. 并在此基础上展现出了优异的耐蚀性能. 该自组装膜在模拟加速磨损试验10 000次后仍具有较好的疏水能力. 这为遥爪型聚合物在固体表面自组装行为的应用提供了新的研究思路.

参 考 文 献

[1] Chen Yuezhen, Pan Yuhong, Pan Yuyi, et al. Ageing behavior analysis of steel structure protection overcoating in marine environment[J]. CoatingsTechnology& Abstracts, 2009, 30(12): 20–22 (in Chinese) [陈月珍, 潘玉红, 潘煜怡, 等. 海洋大气下钢结构保护涂层面漆老化性能分析[J]. 涂料技术与文摘, 2009, 30(12): 20–22]. doi: 10.3969/j.issn.1672-2418.2009.12.009.

[2] Wang Juan, Li Chen, Xu Bo. Basic principle, advance and current application situation of Sol-gel method[J]. Chemical Industry and Engineering, 2009, 26(03): 273–277 (in Chinese) [王娟, 李晨, 徐博. 溶胶-凝胶法的基本原理、发展及应用现状[J]. 化学工业与工程, 2009, 26(03): 273–277]. doi: 10.3969/j.issn.1004-9533.2009.03.020.

[3] Xie Zhenbin. Study of the protective properties of methyl-trimethoxysilicane on historic sandstone[J]. Sciences of Conservation and Archaeology, 2008, 20(4): 10–15,73 (in Chinese) [谢振斌. 甲基三甲氧基硅烷对砂岩石刻封护性能的实验室研究[J]. 文物保护与考古科学, 2008, 20(4): 10–15,73]. doi: 10.16334/j.cnki.cn31-1652/k.2008.04.002.

[4] He Tao, Zhan Xuegui, Shao Yuegang, et al. Optimizing the fabrication of abrasion-resistant and transparent organosilicon coating[J]. Sciencepaper Online, 2007, 2(5): 363–368 (in Chinese) [何涛, 詹学贵, 邵月刚, 等. 有机硅耐磨透明涂料的制备条件优化[J]. 中国科技论文在线, 2007, 2(5): 363–368]. doi: 10.3969/j.issn.2095-2783.2007.05.011.

[5] Wu Zonghan. Progress and application of high performancecorrosion protective coatings[J]. Paint & Coatings Industry, 2007, 37(1): 45–49 (in Chinese) [吴宗汉. 高性能防腐涂料的进展及应用[J]. 涂料工业, 2007, 37(1): 45–49]. doi: 10.3969/j.issn.0253-4312.2007.01.015.

[6] CHEN Mingkai, CHEN Lei, MA Yanjun, et al. Preparation and Protection Mechanism of Anticorrosive Lubricating Coatings[J]. Tribology, 2024, 44(2): 129–142 (in Chinese) [陈明锴, 陈磊, 马彦军, 等. 缓蚀型润滑防腐功能涂层的制备及防护机制研究[J]. 摩擦学学报(中英文), 2024, 44(2): 129–142]. doi: 10.16078/j.tribology.2022264.

[7] ZhuYuguang, NiuShiwei, WangYongguang, et al. Corrosion-wear behavior of polytetrafluoroethylene reinforced chemically bonded phosphate ceramic coatings[J]. Tribology, 2023, 43(5): 572–580 (in Chinese) [朱玉广, 钮市伟, 王永光, 等. 聚四氟乙烯增强氧化铝胶黏陶瓷涂层腐蚀磨损行为[J]. 摩擦学学报, 2023, 43(5): 572–580]. doi: 10.16078/j.tribology.2022005.

[8] LiGuihua, YeYinping, MaYanjun, et al. Preparation of polyamideimide/polytetrafluoroethylene composite coatings and its tribological and anti-corrosion properties[J]. Tribology, 2021, 41(4): 455–466 (in Chinese) [李桂花, 冶银平, 马彦军, 等. 聚酰胺酰亚胺/聚四氟乙烯复合涂层的制备及其摩擦学性能和耐腐蚀性能[J]. 摩擦学学报, 2021, 41(4): 455–466]. doi: 10.16078/j.tribology.2020182.

[9] Luo Yimin, YangJunhua, Li Xia, et al. Self-lubricating and wear-resistant and anti-corrosive multi-functional coating technologies applied in tropical marine atmosphere[J]. Tribology, 2023, 43(1): 104–120 (in Chinese) [罗一旻, 杨军华, 李霞, 等. 热带海洋盐雾气氛自润滑耐磨防腐涂层技术研究新进展[J]. 摩擦学学报, 2023, 43(1): 104–120]. doi: 10.16078/j.tribology.2022032.

[10] Talha M, Ma Yucong, Xu Mingjie, et al. Recent advancements in corrosion protection of magnesium alloys by silane-based Sol–gel coatings[J]. Industrial& EngineeringChemistry Research, 2020, 59(45): 19840–19857. doi: 10.1021/acs.iecr.0c03368.

[11] Yilgör E, Yilgör I. Silicone containing copolymers: Synthesis, properties and applications[J]. ProgressinPolymer Science, 2014, 39(6): 1165–1195. doi: 10.1016/j.progpolymsci.2013.11.003.

[12] Clarson J. , Semlyen J. , Siloxane polymers[B]. 1993.

[13] Palanivel V, Zhu Danqing, van Ooij W J. Nanoparticle-filled silane films as chromate replacements for aluminum alloys[J]. ProgressinOrganic Coatings, 2003, 47(3-4): 384–392. doi: 10.1016/j.porgcoat.2003.08.015.

[14] KumarV B, LeitaoE M. Properties and applications of polysilanes[J]. AppliedOrganometallicChemistry, 2020, 34(3): e5402. doi: 10.1002/aoc.5402.

[15] TalhaM, Ma Yucong, Xu Mingjie, et al. Recent advancements in corrosion protection of magnesium alloys by silane-based Sol–gel coatings[J]. Industrial& EngineeringChemistry Research, 2020, 59(45): 19840–19857. doi: 10.1021/acs.iecr.0c03368.

[16] ItzhaikAlkotzer Y, GrzegorzewskiF, BelausovE, et al. *In situ* interfacial surface modification of hydrophilic silica nanoparticles by two organosilanes leading to stable Pickering emulsions[J]. RSC Advances, 2019, 9(68): 39611–39621. doi: 10.1039/C9RA07597F.

[17] Wu Fan, PickettK, PanchalA, et al. Superhydrophobic polyurethane foam coated with polysiloxane-modified clay nanotubes for efficient and recyclable oil absorption[J]. ACS AppliedMaterials & Interfaces, 2019, 11(28): 25445–25456. doi: 10.1021/acsami.9b08023.

[18] Friesen C M, Améduri B. Outstanding telechelicperfluoropolyalkylethers and applications therefrom[J]. ProgressinPolymer Science, 2018, 81: 238–280. doi: 10.1016/j.progpolymsci.2018.01.005.

[19] Rolland J P, Van Dam R M, Schorzman D A, et al. Solvent-resistant photocurable “liquid teflon”for microfluidic device fabrication[J]. JournaloftheAmerican Chemical Society, 2004, 126(8): 2322–2323. doi: 10.1021/ja031657y.

[20] Renckens T J A, Janeliunas D, van Vliet H, et al. Micromolding of solvent resistant microfluidic devices[J]. Lab on a Chip, 2011, 11(12): 2035. doi: 10.1039/c0lc00550a.

[21] Kim J O, Kim H, Ko D H, et al. A monolithic and flexible fluoropolymer film microreactor for organic synthesis applications[J]. Lab Chip, 2014, 14(21): 4270–4276. doi: 10.1039/c4lc00748d.

[22] Dong Qibao, FuYong, WangHu, et al. Synthesis and characterization of high-performance polymers based on perfluoropolyalkylethers using an environmentallyfriendly solvent[J]. Langmuir, 2020, 36(42): 12513–12520. doi: 10.1021/acs.langmuir.0c01919.

[23] Chen Haijie, Zheng Zhiwen, Yu Hongxiang, etal. Preparation and tribological properties of MXene-based composite films[J]. Industrial& EngineeringChemistry Research, 2021, 60(30): 11128–11140. doi: 10.1021/acs.iecr.1c01588.

[24] ChenHaijie, Qiao Dan, BaZhaowen, et al. Self-assembly and property of perfluoropolyether derivatives lubricating films on glass surface[J]. Tribology, 2019, 39(6): 680–691 (in Chinese) [陈海杰, 乔旦, 巴召文, 等. 玻璃表面全氟聚醚衍生物润滑膜的自组装及性能研究[J]. 摩擦学学报, 2019, 39(6): 680–691]. doi: 10.16078/j.tribology.2019018.

[25] Winnik M A, Yekta A. Associative polymers in aqueous solution[J]. CurrentOpinion in Colloid& Interface Science, 1997, 2(4): 424–436. doi: 10.1016/S1359-0294(97)80088-X.

[26] Berret J F, Calvet D, Collet A, et al. Fluorocarbon associative polymers[J]. CurrentOpinion in Colloid& Interface Science, 2003, 8(3): 296–306. doi: 10.1016/S1359-0294(03)00048-7.

[27] Lo Verso F, Likos C N. End-functionalized polymers: Versatile building blocks for soft materials[J]. Polymer, 2008, 49(6): 1425–1434. doi: 10.1016/j.polymer.2007.11.051.

[28] Tsitsilianis C. Responsive reversible hydrogels from associative “smart” macromolecules[J]. Soft Matter, 2010, 6(11): 2372–2388. doi: 10.1039/B923947B.

[29] Meng Weisheng, He Qun, Yu Manman, etal. Telechelic amphiphilic metallopolymers end-functionalized with platinum(ii) complexes: synthesis, luminescence enhancement, and their self-assembly into flowerlike vesicles and giant flowerlike vesicles[J]. Polymer Chemistry, 2019, 10(32): 4477–4484. doi: 10.1039/c9py00652d.

[30] Berto P, Grelier S, Peruch F. Telechelicpolybutadienes or polyisoprenes precursors for recyclable elastomeric networks[J]. Macromolecular Rapid Communications, 2017, 38(22): 1700475. doi: 10.1002/marc.201700475.

[31] Chen Haiming, Sun Zaizheng, Lin Haohao, etal. Neuron inspired all-around universal telechelicpolyureawith high stiffness, excellent crack tolerance, record-high adhesion, outstanding triboelectricity, and AIE fluorescence[J]. AdvancedFunctionalMaterials, 2022, 32(36): 2204263. doi: 10.1002/adfm.202204263.

[32] Kostov G, Holan M, Ameduri B, etal. Synthesis and Characterizations of Photo-Cross-Linkable Telechelic Diacrylate

Poly(vinylidene fluoride-co-perfluoromethyl vinyl ether) Copolymers[J]. Macromolecules, 2012, 45(18): 7375–7387. doi: 10.1021/ma300932x.

[33] Sehlinger A, Bartnick N, Gunkel I, etal. Phase segregation in supramolecular polymers based on telechelicssynthesized *via*multicomponent reactions[J]. MacromolecularChemistryand Physics, 2017, 218(22): 1700302. doi: 10.1002/macp.201700302.

[34] Reddy K SK, ChenYichun, LinYuan, etal. Synthesis of high-tg, flame-retardant, and low-dissipation telechelicoligo(2, 6-dimethylphenylene ether) resins for high-frequency communications[J]. ACS AppliedPolymerMaterials, 2022, 4(5): 3225–3235. doi: 10.1021/acsapm.1c01792.

[35] Ni Lingli, Dietlin C, Chemtob A, etal. Hydrophilic/hydrophobic film patterning by photodegradation of self-assembled alkylsilanemultilayers and its applications[J]. Langmuir, 2014, 30(33): 10118–10126. doi: 10.1021/la5023938.

[36] Tokudome Y, Hara T, Abe R, etal. Transparent and robust siloxane-based hybrid lamella film As a water vapor barrier coating[J]. ACS AppliedMaterials & Interfaces, 2014, 6(21): 19355–19359. doi: 10.1021/am5054477.

[37] van der Boom M E, Evmenenko G, Dutta P, etal. Nanoscale refractive index tuning of siloxane-based self-assembled electro-optic superlattices[J]. AdvancedFunctionalMaterials, 2001, 11(5): 393–397. doi:10.1002/1616-3028(200110)11: 5<393: AID-ADFM393>3.0.CO;2-S. doi: 10.1002/1616-3028(200110)11:5<393:AID-ADFM393>3.0.CO;2-S.

[38] Fowkes F M. Attractiveforcesatinterfaces[J]. Industrial & Engineering Chemistry, 1964, 56(12): 40–52. doi: 10.1021/ie50660a008.

[39] Voinescu A E, Kellermeier M, Bartel B, etal. Inorganic self-organized silica aragonite biomorphic composites[J]. Crystal Growth & Design, 2008, 8(5): 1515–1521. doi: 10.1021/cg700692t.

[40] Junge F, Lee Pinwei, Kumar Singh A, et al. Interfaces with fluorinated amphiphiles: superstructures and microfluidics[J]. AngewandteChemieInternationalEdition, 2023, 62(12): e202213866. doi: 10.1002/anie.202213866.

[41] Zhang Baofang, Song Jie, Li Dong, et al. Self-assembly of polyoxovanadate-containing fluorosurfactants[J]. Langmuir, 2016, 32(48): 12856–12861. doi: 10.1021/acs.langmuir.6b02308.

[42] Kawauchi T, Kumaki J, Yashima E. Nanosphere and nanonetwork formations of[60]fullerene-end-capped stereoregular poly(methyl methacrylate)s through stereocomplex formation combined with self-assembly of the fullerenes[J]. Journal of the American Chemical Society, 2006, 128(32): 10560–10567. doi: 10.1021/ja063252u.

[43] Guazzelli E, Masotti E, Kriechbaum M, et al. Thermoresponsivereversible unimermicelles of amphiphilic fluorinated copolymers[J]. Macromolecular Chemistry and Physics, 2023, 224(3): 2200360. doi: 10.1002/macp.202200360.

[44] BenderD N, HaitS, LichtenhanJ D, et al. UV curing behavior of five heteroleptic POSS bearing methacrylate and glycidyl groups and evaluation of their potential for hard yet flexible coatings[J]. ACS AppliedPolymerMaterials, 2022, 4(3): 1878–1889. doi: 10.1021/acsapm.1c01702.

[45] Deng Yaling, Sun Jianjun, Ni Xingya, et al. Multilayers of poly(ethyleneimine)/poly(acrylic acid) coatings on Ti_6Al_4V acting as lubricated polymer-bearing interface[J]. JournalofBiomedicalMaterials Research Part B: AppliedBiomaterials, 2020, 108(5): 2141–2152. doi: 10.1002/jbm.b.34553.

[46] Cai Yongwei, Zhao Qi, Quan Xuejun, et al. Corrosion-resistant hydrophobic MFI-type zeolite-coated mesh for continuous oil–water separation[J]. Industrial& EngineeringChemistry Research, 2020, 59(8): 3498–3510. doi: 10.1021/acs.iecr.9b05923.

[47] Hao Zhentao, Chen Chuchu, Shen Ting, et al. Slippery liquid-infused porous surface *via* thermally induced phase separation for enhanced corrosion protection[J]. JournalofPolymer Science, 2020, 58(21): 3031–3041. doi: 10.1002/pol.20200272.

[48] Zhang Y. , Tang S. , Hu J. , et al. Formation mechanism and corrosion resistance of the hydrophobic coating on anodized magnesium[J]. Corrosion Science: 2016, 111, 334-343. doi:10.1016/j.corsci.2016.05.023.